Biomed Microdevices (2014) 16:639–644
DOI 10.1007/s10544-014-9866-0

Quasi-digital PCR: Enrichment and quantification of rare DNA variants

Scott O. Sundberg · Carl T. Wittwer · Luming Zhou · Robert Palais · Zachary Dwight · Bruce K. Gale

Published online: 1 May 2014

Abstract Rare variant enrichment and quantification was achieved by allele-specific, competitive blocker, digital PCR for aiming to provide a noninvasive method for detecting rare DNA variants from circulating cells. The allele-specific blocking chemistry improves sensitivity and lowers assay cost over previously described digital PCR methods while the instrumentation allowed for rapid thermal cycling for faster turnaround time. Because the digital counting of the amplified variants occurs in the presence of many wild-type templates in each well, the method is called "quasi-digital PCR". A spinning disk was used to separate samples into 1000 wells, followed by rapid-cycle, allele-specific amplification in the presence of a molecular beacon that serves as both a blocker and digital indicator. Monte Carlo simulations gave similar results to Poisson distribution statistics for mean number of template molecules and provided an upper and lower bound at a specified confidence level and accounted for input DNA concentration variation. A 111 bp genomic DNA fragment including the *BRAF* p.V600E mutation (c.T1799A) was amplified with quasi-digital PCR using cycle times of 23 s. Dilution series confirmed that wild-type amplification was suppressed and that the sensitivity for the mutant allele was <0.01 % (43 mutant alleles amongst 500,000 wild-type alleles). The Monte Carlo method presented here is publically available on the internet and can calculate target concentration given digital data or predict digital data given target concentration.

Keywords Digital PCR · Microfluidics · Allele-specific PCR

1 Introduction

Detection of rare DNA variants such as circulating tumor cells (Ashworth 1869) has the potential to provide a noninvasive, sensitive technique to detect cancer earlier and provide information for proper therapy selection and drug resistance. Cell enrichment approaches have been applied to address the low concentration of circulating tumor cells (Nagrath et al. 2007) but can suffer from low specificity, low sensitivity, a loss of target cells, or false negatives and positives (Alunni-Fabbroni and Sandri 2010).

PCR based techniques have been developed to address sensitivity and specificity issues that have arisen from cell enrichment approaches. One such technology that has improved sensitivity is BEAMing (beads, emulsion, amplification and magnetics); finding mutated circulating free DNA in plasma of colorectal cancer patients (Diehl et al. 2008; Dressman et al. 2005). Another PCR technique used is the amplification refractory mutation system (Newton et al. 1989), providing allele-specific amplification. To further improve on this primer design, allele-specific competitive blocker-polymerase chain reaction has been implemented (Orou et al. 1995), providing a 'double kill' methodology to preferentially amplify the mutant template. A blocker is

Electronic supplementary material The online version of this article (doi:10.1007/s10544-014-9866-0) contains supplementary material, which is available to authorized users.

S. O. Sundberg · C. T. Wittwer · L. Zhou · Z. Dwight
Department of Pathology, University of Utah,
15 North Medical Drive East, Salt Lake City, UT 84112, USA

R. Palais
Department of Mathematics, University of Utah,
155 S 1400 E Room 233, Salt Lake City, UT 84112, USA

B. K. Gale
Department of Mechanical Engineering, University of Utah,
50 S Central Campus Dr MEB 2110, Salt Lake City, UT 84112, USA

S. O. Sundberg (✉)
9800 Medical Center Drive, Rockville, MD 20850, USA
e-mail: scott.sundberg@path.utah.edu

designed to match the more common template for suppression during PCR. In addition, one primer is matched to the mutant template for allele-specific PCR. This method greatly delays amplification of the more common template. Recent implementation of this method has used a probe as both the wild-type blocker and to detect the mutant allele for a rapid, closed tube technique (Zhou et al. 2011).

Digital PCR (Vogelstein and Kinzler 1999) has the potential to improve limits of detection, using limiting dilution or volume to detect minor fractions of mutated DNA and analyzing binary positive/negative calls. When digital PCR is combined with allele-specific PCR, 0.02 % of a variant sequence can be detected (Whitcombe et al. 1999; Wang et al. 2010). This combination method, "quasi-digital PCR", selectively amplifies the mutation allele within a background of wild-type DNA and detects only the mutation allele.

Typically the number of positive reactions with digital PCR is correlated to the mean number of copies present using the Poisson approximation, as this method is easy to implement and provides an accurate estimate. In addition, binomial probability (Dube et al. 2008) or the score method (Shen et al. 2010) can be used to provide a confidence interval for the number of copies present.

The focus of this work is to achieve a more rapid, less expensive process for quasi-digital PCR with capability for lower limits of detection. The assay methodology can be implemented across any digital PCR platform to further improve limits of detection. A custom statistical analysis tool was developed to improve copy number quantification of digital PCR experiments using Monte Carlo simulation for comparison to the Poisson approximation.

2 Materials and methods

2.1 Disk design and manufacturing

The digital PCR disk design has been described previously (Sundberg et al. 2010). In brief, the disk compartmentalizes sample into 1000 individual wells, with each well containing a mean volume of 33 nl, using centrifugal force (Fig. 1). The disk patterning process is similar but materials and thin-film plastic bonding have changed for this work. An FR83-Black polycarbonate thin film sheet, 125 μm thick, (Sabic Polymer shapes, Fresno, CA) was patterned with the loading reservoir, spiral channel and 1000 wells. This sheet was then thermally bonded between two other FR83-Clear polycarbonate thin film sheets (Sabic Polymer shapes) of the same thickness, laminating the plastic layers together at 175 °C for 2 min using a Jet Press 14 heat press (Geo Knight, Brockton, MA).

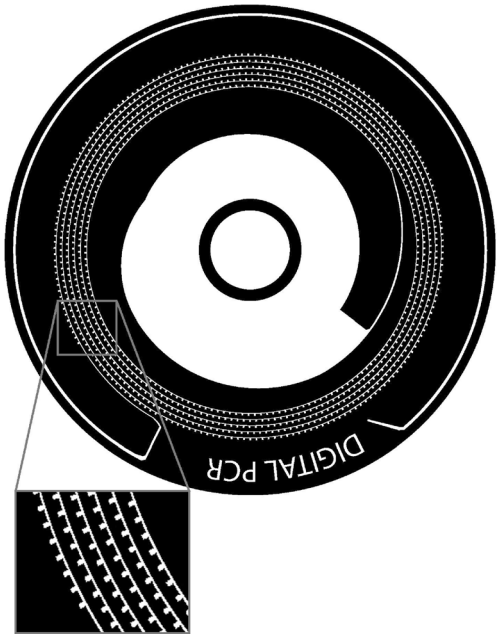

Fig 1 Spinning disk for digital PCR. The disk consists of a loading reservoir, spiral microchannel with 1000 wells facing radially outward along the channel, and an overflow channel at the edge of the disk

2.2 Allele-specific PCR design

Allele-specific, competitive blocker, polymerase chain reaction utilizes a 'double kill' technique to preferentially amplify the mutation allele by utilizing a primer that matches the mutation allele while refractory to wild-type and a probe designed to match the wild-type to further inhibit primer annealing on the wild-type allele (Fig. 2). The forward primer 5' GTGATTTTGGT-CTAGCTACAGA 3' and reverse primer 5' TCAGTGGAAAAATAGCCTCAATTC 3' were designed to amplify a 111 bp product from the mutant allele. The competitive blocker probe used was the molecular beacon probe 5' FAM-CGGTCTAGCTAC-AGTGAAATCTCGAC CG–BHQ 3' (Biosearch Technologies, Novato, CA). The bolded nucleotides in the forward primer and molecular beacon probe sequences represent the location of the mutation site for T1796A *BRAF*, a known mutation site prevalent in malignant melanomas (Yazdi et al. 2003) and papillary thyroid cancer (Xing et al. 2004) and can also be found within other cancers (Davies et al. 2002).

2.3 PCR preparation

Wild-type human genomic DNA was extracted from human blood and the *BRAF* homozygous mutation was obtained from the ATCC as purified DNA (HTB-72D, American Type Culture Collection, Manassas, VA). The concentrations of genomic DNA were determined by absorbance at 260 nm (A_{260}), assuming an A_{260} of 1.0 is 50 μg/mL.

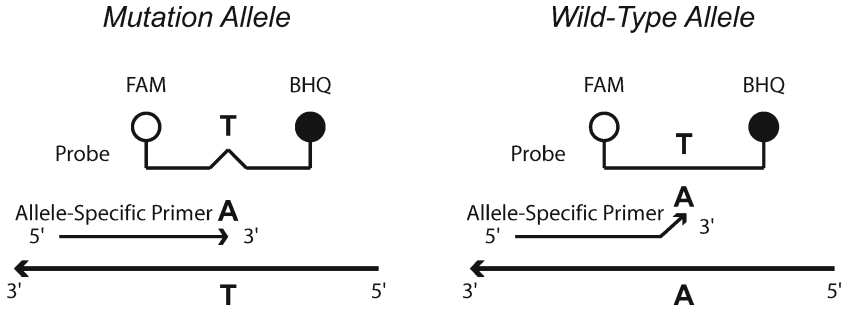

Fig 2 Allele-specific, competitive-blocker PCR for enrichment of minor mutation alleles. The allele-specific primer is matched to the mutation allele at its 3'-base, while mismatched to the wild-type allele. In addition, a molecular beacon probe is matched to the wild-type allele and mismatched to the mutation allele, resulting in competitive blocking of the primer and favoring amplification of the mutation allele. The probe also acted as the detection signal of the digital PCR reaction. FAM=5'-fluorescein label. BHQ=Black hole quencher

The PCR mixture comprised *BRAF* mutation DNA, ranging from 0.5 to 0.005 μg/mL, as the template with 1 μM reverse primer, 0.2 μM forward primer, 0.5 μM molecular beacon probe, 200 μM of each deoxynucleotide triphosphate (dNTP), 40 U/mL of KlenTaq1 polymerase (AB Peptides, St. Louis, MO), 6.4 μg/mL of Anti-Taq Monoclonal Antibody (eENZYME, Montgomery Village, MD), 2 mM $MgCl_2$, and 1X LCGreen Plus (Idaho Technology, Salt Lake City, UT) in 50 mM Tris (pH 8.3), 500 μg/mL BSA, and 2.5 % polyvinylpyrrolidone (PVP) (Av. Mol. Wt. 360,000, Sigma-Aldrich Corporation, St. Louis, MO). Tests involving a mixture of mutation and wild-type DNA also contained 50 μg/mL wild-type DNA.

Forty μL of PCR mix and 100 μL of mineral oil (M5904, Sigma-Aldrich Corporation), dyed with 1 mg/mL Oil Red O (Matheson Coleman & Bell, Gardena, CA), were pipetted into the disk loading reservoir. Two polycarbonate disks, 750 μm thick with an outer diameter of 75 mm, were then coupled to each side of the disk. The disk was spun for 5 min at 4500 rpm to load each of the wells along the spiral channel path and to fill the channel with mineral oil. The end of the spiral channel was then thermally sealed prior to thermocycling to create a closed system.

2.4 Thermocycling

The disk rapid air thermocycling instrument has been described previously (Sundberg et al. 2010; Wittwer et al. 1997). Briefly described, the thermocycler consisted of an air chamber with rapid convection heating and cooling, a thermocouple within the air chamber for temperature feedback, and a servo motor that rotated the microfluidic disk continuously during thermocycling. For disks containing only mutation template, 100 cycles of 50 °C annealing for 0 s hold, 72 °C extension for 2 s hold, and 95 °C denaturing for 0 s hold was achieved in about 45 min while spinning the disk at 4500 rpm (27 s/cycle). The annealing temperature was raised for disks that contained mutation template with wild-type background to prevent wild-type amplification, with 100 cycles of 55 °C annealing for 0 s hold, 72 °C extension for 2 s hold, and 95 °C denaturing for 0 s hold in about 38 min (23 s/cycle).

2.5 Disk imaging and analysis

The disk was fluorescently imaged following PCR for digital well analysis. This consisted of a 470 nm blue LED positioned 70 mm below the disk with an excitation filter of 469 DF35 (FF01-469/35-25, Semrock, Rochester, NY). The excitation light source was mounted on a turntable with the LED located 45 mm from its center. This turntable was rotated by a stepper motor (PK266-01A, Oriental Motor, Torrance, CA) controlled using an MID 7604 motor driver and PCI 7330 card (National Instruments, Austin, TX). The excitation light was rotated one revolution during imaging at a velocity of 10 rpm to achieve more uniform excitation over all of the wells within the disk. The emitted fluorescent light from the disk wells was collected with a lens (Ultrasonic EF 20 mm 1:2.8, Canon, Tokyo, Japan) positioned 350 mm above the center of the disk. This collected light then passed through a 525 DF20 bandpass filter (FF01-525/20-25, Semrock) and was imaged with a CCD camera (iXon, Andor Technology, South Windsor, CT) cooled to −20 °C. Andor iXon software version 4.0 (Andor Technology) was used to take a 45 s exposure background subtraction image followed by a 45 s exposure (Fig. 3). The image threshold was set from 0–2500, saved as a jpg file, and imported into the U.S. National Institutes of Health's ImageJ software (http://rsb.info.nih.gov/ij/) for analysis. This software was then used to threshold, size exclude, and create histograms of well intensity for each disk image. The threshold and minimum pixel number was user defined in the software. Histogram frequency distributions determined the number of positive and negative wells for each test with normal distribution curves fitted to the histogram data using Minitab 15 statistical software (Minitab, State College, PA). The intersection of the two normal distribution fitted curves determined the cut-off point for positive and negative calls.

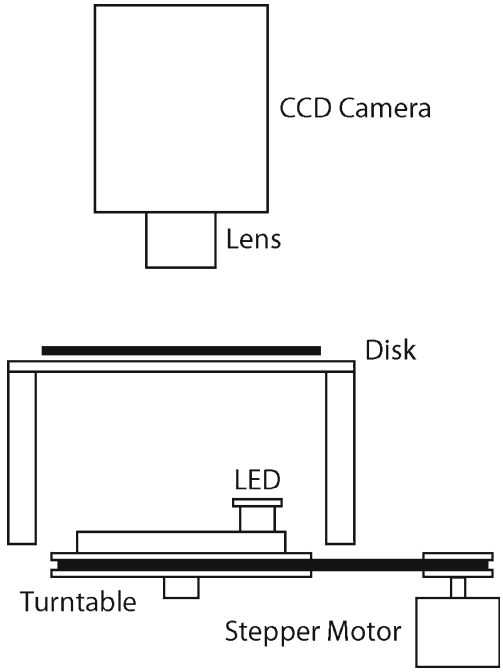

Fig 3 Configuration for disk imaging. The entire disk was imaged while a rotating LED illuminated the ring of digital PCR samples for homogeneity

2.6 Statistical analysis

Two statistical analysis approaches were compared. The first method determines the number of copies amplified using Poisson approximation. The second method uses a Monte Carlo approach to simulate digital PCR outcomes of thousands of different scenarios using LabVIEW's (National Instruments) random number generator. This approach provides an accurate representation of copy numbers amplified for a given positive well count, which can be used to verify the Poisson approximation, and can also provide confidence interval information. The Library Generator performs this Monte Carlo simulation task to create a library that is then called up by uCount^{SM} software for interpretation. This software is a presentation tool for the simulated data and is offered as a public service (http://www.dna.utah.edu/ucount/uc.html). These two custom software programs are described in more detail.

2.6.1 Library generator

An input copy number is simulated to account for variation that occurs within DNA sample concentration. This simulation is performed 10,000 times to create a frequency histogram centered at the mean input concentration for normal distribution histograms (asymmetric distributions exist as the input copy number approaches one copy). For each input copy number simulated another random number generator is used to distribute the input copies randomly across the specified number of wells of the predefined library such that multiple copies can reside within the same well. The library generator then saves a text file format with a 2D array of histograms showing positive well frequency for each mean input copy number simulated.

2.6.2 uCount^{SM} (Monte Carlo)

The library created with the Library Generator is then imported into uCount^{SM} where two options are available; analysis (Supplementary Fig. 1a) and prediction (Supplementary Fig. 1b). In analysis mode the user selects the library desired, based on the number of wells of the digital PCR experiment. The user then inputs the number of positive wells and specifies a confidence level. uCount^{SM} outputs a histogram and provides the mean copies present with an upper and lower bound interval which corresponds to the confidence level. Under the prediction mode the user selects the library, inputs the mean copy count and confidence level. uCount^{SM} then outputs the mean positive wells that would occur, with an upper and lower bound interval corresponding to the confidence level.

3 Results and discussion

Standard digital PCR within the spinning disk was first demonstrated with a dilution series of pure *BRAF* mutation DNA (Fig. 4). The dilution series ranged from 0.5 to 0.005 μg/mL, or 5 to 0.05 copies/well. Another dilution series was then performed using *BRAF* mutation DNA within a larger wild-type background to demonstrate quasi-digital PCR. The *BRAF* mutation concentration again ranged from 0.5 to 0.005 μg/mL while the wild-type background was held constant at 50 μg/mL or 500 copies/well (Fig. 4). The allele-specific chemistry effectively suppressed wild-type amplification, giving similar results by both methods. There is some variation in the apparent intensity of both positive and negative peaks that results from variable user-defined brightness and contrast settings for each run.

Table 1 provides the number of positive wells within each disk as well as the number of mutant template copies calculated by either the Poisson approximation or by Monte Carlo simulation. The 95 % confidence interval is also given for the Monte Carlo simulations. Both methods agree closely. Predicted positive wells from the prediction mode of uCount^{SM} software are also provided at a 95 % confidence level.

T1796A *BRAF* mutation DNA was successfully amplified and digitally analyzed on the spinning disk with and without 500 wild-type background copies per well. A sensitivity for the mutant allele <0.01 % was achieved. Not all wells fluoresced at the highest target concentrations, consistent with Poisson calculations and Monte Carlo simulations. For

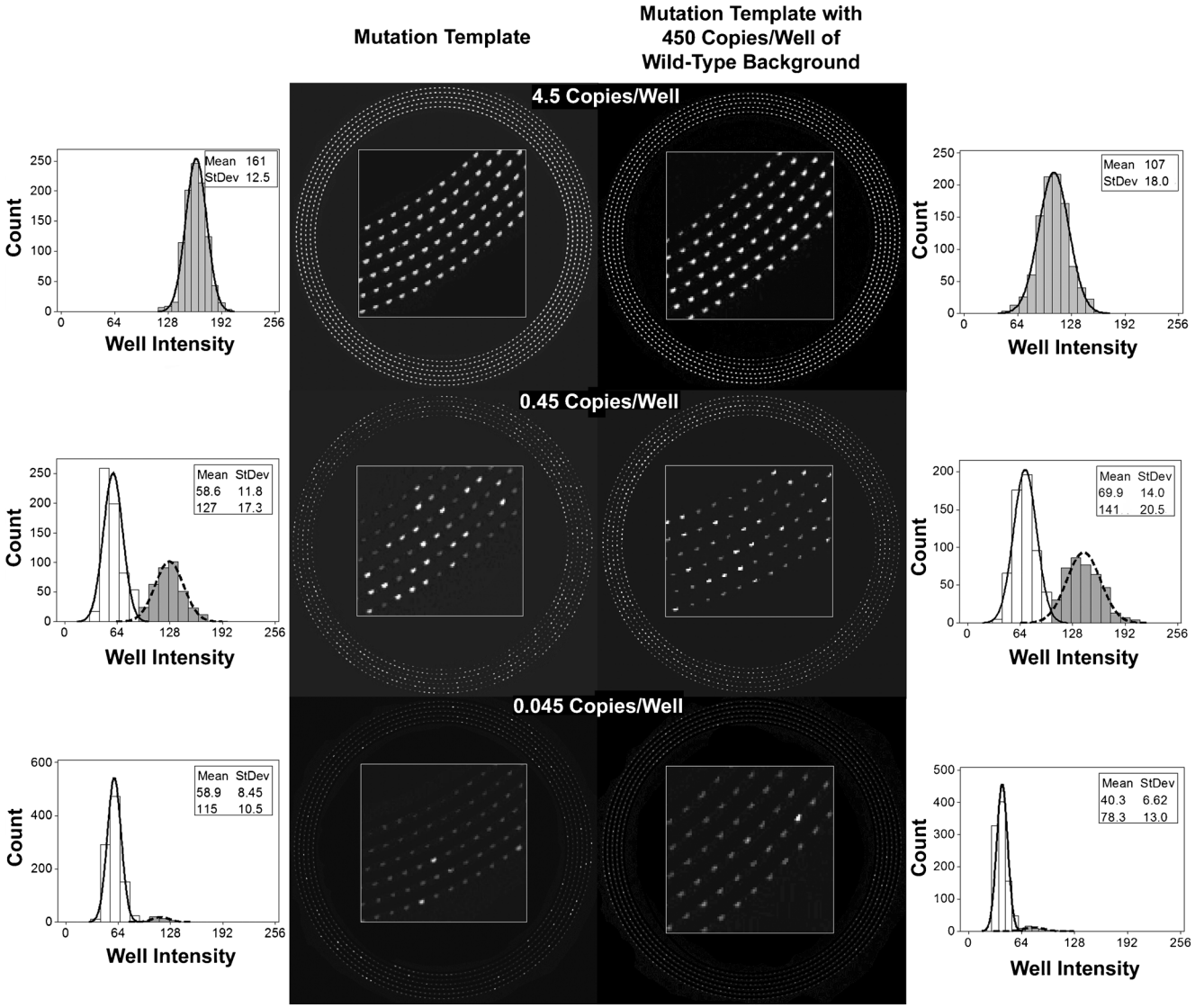

Fig 4 Digital PCR fluorescent images from 5, 0.5, and 0.05 copies/well of *BRAF* mutation DNA (Left) and *BRAF* mutation DNA (5, 0.5, and 0.05 copies/well) admixed with wild-type background DNA at 500 copies/well (Right). Histogram data corresponding to each image is also presented. Positive and negative distributions are fit to Gaussian curves, and the mean and standard deviation of each are listed

example, with an average concentration of 5 copies per well there is approximately a 1 % chance that a well does not have any mutation DNA present, similar to observation (Table 1).

The human genomic DNA concentration determined by absorbance correlates well to the copy number predictions determined by digital PCR. For example, at 0.05 copies/well determined by absorbance and dilution, the average result by digital PCR was 0.0435 copies/well (n=4). At 0.5 copies/well input, the average by digital PCR was 0.51 (n=4), and at 5 copies per well, the average by digital PCR was 5.2 (n=4). A couple of data points lied outside the predicted positive well count. Observed errors can be either systematic or random. Possible systematic errors include those from the absorbance measurement, volume errors during dilution, and estimates of the well volume. For example, the number of positive wells for the dilution series with wild-type background was in general higher than without background DNA (Table 1). Random errors are expected from the stochastic nature of digital PCR and this variance can be estimated by Poisson or Monte Carlo methods as shown here. Random errors increase as the percent of positive wells approach either 0 or 100 % where the variance expected from digital PCR expands rapidly.

A detection rate <0.01 % was achieved based on an average of 43 mutation copies among 500,000 wild-type copies across three individual tests. This detection is a factor of two better than previously published quasi-digital PCR, although the background copy number used in this study was nearly three orders of magnitude greater (500 copies/well compared to 6–7 copies/well). The limit of detection could approach ~0.001 % using the current chemistry and well configuration by diluting

Table 1 Summary statistics for two template dilution series on the spinning PCR disk

DNA concentration			Mutation template			Mutation template with 500 Copies/Well of wild-type background		
Copies/Well	Copies/Disk	Positive wells predicted[b]	Positive wells	Copies present		Positive wells	Copies present	
				Poisson[c]	Monte Carlo[d]		Poisson[c]	Monte Carlo[d]
5	5000	N/A[e]	992	4828	N/A[e]	996	5521	N/A[e]
0.5[a]	500	394 (364–424)	384	485	484 (438–535)	389	493	492 (444–543)
						402	514	514 (466–567)
						425	553	553 (502–607)
0.05[a]	50	49 (37–64)	42	43	43 (31–57)	34	35	34 (24–48)
						45	46	46 (33–61)
						49	50	50 (37–65)

a. This DNA concentration was tested in triplicate when wild-type background DNA was added

b. Positive wells expected using the prediction mode of uCount[SM] at a 95 % confidence level

c. Mean copy number based on Poisson approximation. Calculated as -ln (proportion negative wells)*(number of wells)

d. Mean copy number based on Monte Carlo simulations performed with uCount[SM]. A lower and upper bound at a 95 % confidence level is also provided

e. Libraries currently generated for uCount[SM] software not valid at this high of a percentage of positive wells

the mutation sample with the same high concentration of wild-type background.

Quasi-digital PCR quantification results with rapid PCR thermocycling were obtained in about an hour. Thermal cycle times (23 s) were much faster than prior allele-specific PCR using scorpion primers (>90 s cycles), which also required a 10 min hot start (Wang et al. 2010). Although our technique used twice as many cycles, the total PCR time was still less than half the time typical for standard PCR. Furthermore, by eliminating scorpion primers assay costs have been reduced.

Monte Carlo simulations show that the Poisson approximation does provide an accurate mean copy number calculation. The web simulation provides an accurate and user friendly tool to display the expected distribution of template concentrations, given a digital PCR result. Conversely, given a DNA template concentration, the distribution of expected digital PCR results is displayed. Due to the availability of the entire distribution for analysis and prediction modes one can understand to what degree results are normally or asymmetrically distributed. Upper and lower bounds at 90, 95, and 99 % can be selected for either digital analysis or prediction, even as the number of positive wells approaches 0 or 100 %.

Acknowledgments The authors thank the University of Utah Research Foundation and the Utah Science Technology and Research initiative (USTAR) in conjunction with the American Recovery and Reinvestment Act (ARRA) for kindly supporting this work. We also thank Carl Wittwer's lab group and Bruce Gale's lab group for valuable advice pertaining to this research.

Conflicts of interest Authors Scott Sundberg, Carl Wittwer and Bruce Gale hold patent rights pertaining to the spinning disk technology used in this work. The authors declare that they have no other conflicts of interest.

References

M. Alunni-Fabbroni, M.T. Sandri, Methods **50**, 289–297 (2010)
T.R. Ashworth, Aust. Med. J. **14**, 146–149 (1869)
H. Davies, G.R. Bignell, C. Cox, P. Stephens, S. Edkins, S. Clegg, J. Teague, H. Woffendin et al., Nature **417**, 949–954 (2002)
F. Diehl, K. Schmidt, M.A. Choti, K. Romans, S. Goodman, M. Li, K. Thornton, N. Agrawal et al., Nat. Med. **14**, 985–990 (2008)
D. Dressman, H. Yan, G. Traverso, K.W. Kinzler, B. Vogelstein, Proc. Natl. Acad. Sci. U. S. A. **102**, 16368–16373 (2005)
S. Dube, J. Qin, R. Ramakrishnan, PLoS ONE **3**, e2876 (2008)
S. Nagrath, L.V. Sequist, S. Maheswaran, D.W. Bell, D. Irimia, L. Ulkus, M.R. Smith, E.L. Kwak et al., Nature **450**, 1235–1241 (2007)
C.R. Newton, A. Graham, L.E. Heptinstall, S.J. Powell, C. Summers, N. Kalsheker, J.C. Smith, A.F. Markham, Nucleic Acids Res. **17**, 2503–2515 (1989)
A. Orou, G. Fechner, G. Utermann, H.J. Menzel, Hum. Mutat. **6**, 163–169 (1995)
F. Shen, W. Du, J.E. Kreutz, A. Fok, R.F. Ismagilov, Lab Chip **10**, 2666–2672 (2010)
S.O. Sundberg, C.T. Wittwer, C. Gao, B.K. Gale, Anal. Chem. **82**, 1546–1550 (2010)
B. Vogelstein, K.W. Kinzler, Proc. Natl. Acad. Sci. U. S. A. **96**, 9236–9241 (1999)
J. Wang, R. Ramakrishnan, Z. Tang, W. Fan, A. Kluge, A. Dowlati, R.C. Jones, P.C. Ma, Clin. Chem. **56**, 623–632 (2010)
D. Whitcombe, J. Theaker, S.P. Guy, T. Brown, S. Little, Nat. Biotechnol. **17**, 804–807 (1999)
C.T. Wittwer, K.M. Ririe, R.V. Andrew, D.A. David, R.A. Gundry, U.J. Balis, BioTech. **22**, 176–181 (1997)
M. Xing, V. Vasko, G. Tallini, A. Larin, G. Wu, R. Udelsman, M.D. Ringel, P.W. Ladenson, D. Sidransky, J. Clin, Endocrinol. Metab. **89**, 1365–1368 (2004)
A.S. Yazdi, G. Palmedo, M.J. Flaig, U. Puchta, A. Reckwerth, A. Rütten, T. Mentzel, H. Hügel et al., J. Investig. Dermatol. **121**, 1160–1162 (2003)
L. Zhou, Y. Wang, C.T. Wittwer, BioTech. **50**, 311–318 (2011)